Abstract

213

Development of a Probody Drug Conjugate (PDC) Targeting EpCAM for the Treatment of Solid Tumors

Yimao Liu[1], Rui Wu[1], Cristina Gavrilescu[1], Jason Sagert[2], Kimberly Tipton[2], Shouchun Liu[2], Chanty Chan[2], Steven Boulé[1], Alan Wilhelm[1], Jacquelynn Lucas[1], Bahar Matin[1], Jean-Michel Lecerf[1], Marian Themeles[1], Ashley Morneault[1], Tara Drake[1], Sadiqa Yancey[1], Neeraj Kohli[1], Christopher Espelin[1], John Follit[1], Kerry A. Donahue[1], Thomas Chittenden[1], Cynthia Guidi[1], Stuart W. Hicks[1]

[1]ImmunoGen, Inc., Waltham, MA; [2]CytomX Therapeutics, Inc., South San Francisco, CA

INTRODUCTION

- EpCAM (Epithelial Cell Adhesion Molecule) is a glycosylated,~40-kDa, type I transmembrane protein playing a role in both tumor and cancer stem cell biology
- Overexpression of EpCAM on a wide variety of adenocarcinomas, including on cancer-initiating/cancer cells, makes it a very attractive target for an antibody drug conjugate (ADC) approach. However, high expression on normal tissues has limited development of EpCAM-targeted therapies due to safety concerns
- Probody™ technology developed by CytomX Therapeutics allows for the selection of targets that were thought to be incompatible with ADC development due to high normal tissue expression
- An EpCAM-specific Probody drug conjugate (PDC) may provide the tumor killing efficacy of an EpCAM-targeting ADC while limiting the on-target toxicity as a result of normal tissue expression of EpCAM
- An anti-EpCAM PDC represents a promising therapeutic strategy to target a wide range of EpCAM-expressing tumors

Probody™ technology allows for tumor-selective antigen binding

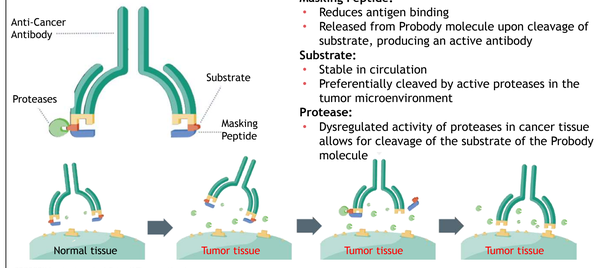

Masking Peptide:
- Reduces antigen binding
- Released from Probody molecule upon cleavage of substrate, producing an active antibody

Substrate:
- Stable in circulation
- Preferentially cleaved by active proteases in the tumor microenvironment

Protease:
- Dysregulated activity of proteases in cancer tissue allows for cleavage of the substrate of the Probody molecule

PROBODY is a trademark of CytomX Therapeutics, Inc.

EpCAM is highly expressed in multiple tumor indications

IHC analysis of EpcAM expression in tumor microarrays

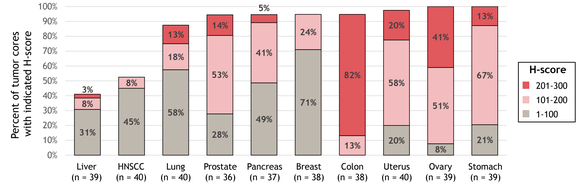

Generation of EpCAM-targeting Probody molecules

- A panel of Probody molecules was generated based on a novel cynomolgus-cross reactive, humanized anti-EpCAM antibody
  - Masking peptides were identified from peptide libraries using bacterial display technology
  - Selected masking peptides were genetically fused to the parental antibody via a protease-cleavable linker
  - Binding of the intact (masked) EpCAM-targeting Probody molecules to EpCAM-expressing cells was dramatically reduced; *in vitro* activation with uPA (urokinase-type plasminogen activator) restored binding affinity comparable to the parental antibody

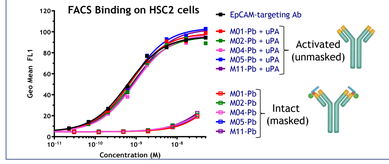

Mask	ELISA KD (nM)	Mask Efficiency
-	0.35	-
M01	35	100
M11	20	53
M05	16	44
M04	11	31
M07	10	27
M03	9	25
M02	7	19

In vitro and *in vivo* evaluation of anti-EpCAM PDC masks

Inhibition of *in vitro* activity of anti-EpCAM PDCs correlates with mask efficiency

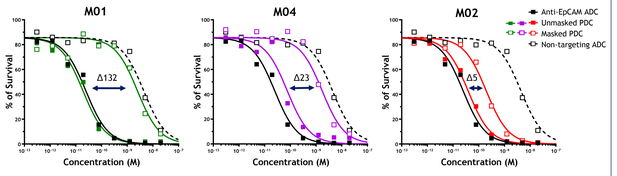

- EpCAM-targeting Probody molecules were successfully conjugated with multiple cytotoxic linker/payloads
- M03, M04, M05 and M07 DGN549 PDCs had similar activity and specificity

EpCAM-DGN549 PDCs are active in the NCI-H2110 NSCLC xenograft model

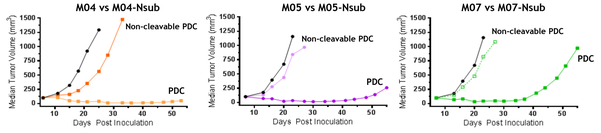

- M04, M05 and M07-DGN549 PDCs showed promising activity at 0.25 mg Ab/kg
- The non-cleavable PDC comparators (lacking protease substrates) were inactive at this dose
- M05 gave more CR and biggest window between non-cleavable and cleavable DGN549 PDCs and was selected for further evaluation

M05-DM4 PDC is potent against various EpCAM-positive cell lines

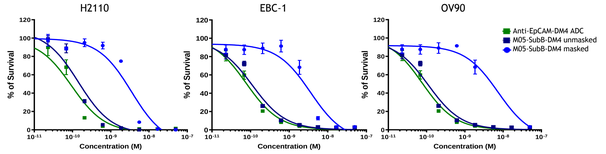

- All three cell lines are sensitive to anti-EpCAM-DM4 ADC
- Unmasked M05-DM4 PDC had similar potency as the ADC
- The specific windows between unmasked and masked PDCs are ≥25-fold

M05-DM4 PDC is active in multiple xenograft models

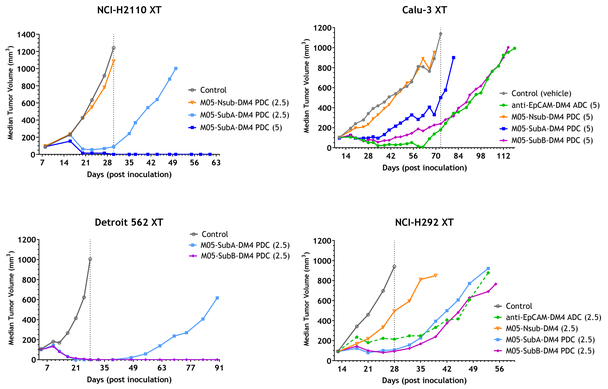

Shown: Single dose treatments administered based on Ab dose. Dose as indicated (mg/kg).

- **The DM4 PDC is highly efficacious across multiple tumor models**
  - The activity is similar to that of the corresponding ADC

M05-DM4 PDCs have improved tolerability & PK profiles relative to the EpCAM ADC in cynomolgus monkeys

M05-DM4 PDCs were tolerated at a higher dose than the ADC

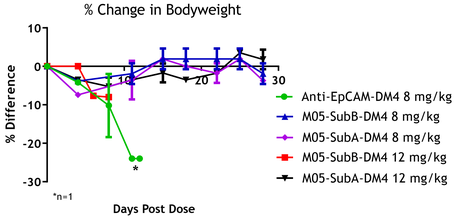

- Clinical observations were more severe in the ADC group resulting in moribund condition
- A difference in tolerability was noted between two different substrates
  - The two substrates differ in their susceptibility to cleavage by different proteases

M05-DM4 PDCs had longer half-lives and exposures than the ADC

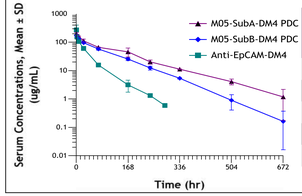

TK parameters (Mean ± SD)	8 mg/kg dose		
	M05-SubA-DM4 PDC	M05-SubB-DM4 PDC	Anti-EpCAM-DM4 ADC
AUC∞ (hr*µg/mL)	19000 ± 61.1	13600 ± 874	5510 ± 947
C_{max} (µg/mL)	200 ± 20.8	177 ± 3.82	275 ± 134
Cl (mL/hr/kg)	0.421 ± 0.001	0.59 ± 0.04	1.47 ± 0.25
$T_{1/2}$ (hr)	94.9 ± 12.4	64.3 ± 16.9	33.9 ± 6.39
V_{ss} (mL/kg)	56.6 ± 3.39	58.2 ± 5.33	53.3 ± 3.12

CONCLUSIONS

- A panel of PDCs targeting EpCAM was developed
- The antigen binding and *in vitro* cytotoxicity of intact PDCs were significantly reduced compared to that of the corresponding ADCs, but can be restored following *in vitro* proteolytic activation
- We demonstrated that an EpCAM PDC has potent activity in *in vivo* efficacy models as well as improved tolerability and exposure relative to an EpCAM ADC

An EpCAM-targeting PDC represents a promising therapeutic candidate to target a wide range of EpCAM-expressing tumors

AACR Annual Meeting March 29th to April 3rd 2019 in Atlanta, Georgia

Generation of site-specific DARPin® drug conjugates using EGFR as a model system

Abstract 215

Laura A. Laviolette[1], Cynthia J. Guidi[1], Christian Reichen[2], Qifeng Qiu[1], Luke Harris[1], Patricia Schildknecht[2], Stefanie Fischer[2], Zita Arany[2], Tanja Hospodarsch[2], Anna Skaletskaya[1], Megan Fuller[1], Stephen Abbott[1], Rebecca McCarthy[1], Jenny Lee[1], Katherine Francisco[1], Kerstin Sinkevicius[1], Sharlene Adams[1], Christopher Espelin[1], Emily Reid[1], Wei Li[1], Carla Marashio[1], Kerry Donahue[1], Stuart Hicks[1], and Dan Snell[2]

Affiliations: [1]ImmunoGen, Inc, Waltham MA, USA and [2]Molecular Partners AG, Zurich, Switzerland

INTRODUCTION

DARPin® molecules are small engineered proteins, derived from natural ankyrin repeat proteins, that are selected to bind to specific targets with high affinity. Individual DARPin® molecules can be linked together genetically in order to create multi-specific drug molecules. The versatility of DARPin® molecules makes them an attractive alternative to antibodies for the development of drug conjugates. We have developed two DARPin® drug conjugates (DDCs) targeting a known tumor associated antigen, epidermal growth factor receptor (EGFR), as a model system. Two different EGFR DDCs were generated using EGFR-binding DARPin® molecules with different binding affinities. A control DDC using a non-targeting DARPin® molecule was also generated. Each of the multi-DARPin® molecules consisted of four DARPin® modules, including half-life extension domains, and had a total molecular weight of approximately 60kDa. The multi-DARPin® constructs were conjugated to the indolinobenzodiazepine mono-imine DGN549, a potent DNA alkylating payload. DDCs were evaluated for binding and direct cytotoxicity following conjugation. The *in vivo* stability and efficacy of the DDCs were also evaluated. The modularity of DARPin® molecules combined with the potency of the DGN549 payload allows for the production of highly active targeted anti-cancer conjugates.

Multi-DARPin® constructs utilizing different EGFR binding domains

- EGFR-targeting DARPin® molecules consisting of four mono-DARPin® domains, including serum albumin (SA)-binding DARPin® domains for half-life extension, were generated. A non-targeting DDC was also generated.

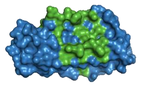

Schematic representation of a DARPin® binding domain

DARPin® Molecule		*hEGFR K_d [nM]	*mEGFR K_d [nM]
anti-EGFR DARPin® 1	PSC099	0.02	0.4
anti-EGFR DARPin® 2	PSC106	0.08	2.3
Non-binding (NB) DARPin®	PSC108	Non-binding	

*SPR binding of monovalent EGFR molecules

- Two different EGFR targeting DARPins® (red and blue) were evaluated

EGFR-binding DARPin® molecules internalize and co-localize with the lysosomal marker Lamp1

- EGFR-binding DARPins® bind to EGFR expressing tumor cells, are internalized and delivered to lysosomes
  - DARPin® molecules directly-labelled with AF568 were bound to SKOV3 cells for 1 hr on ice (0 hrs time point) and then incubated at 37°C for 48 hrs. Co-localization with the lysosomal membrane protein, Lamp1, was assessed using an anti-Lamp1 AF488 antibody

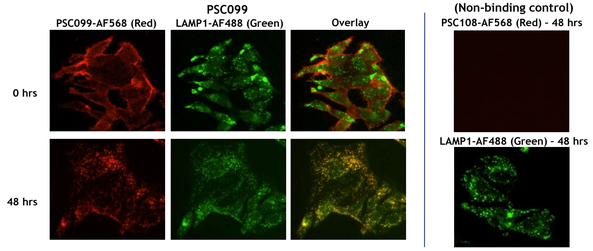

DARPin® molecules have favorable conjugation properties with the potent DNA alkylator DGN549

- DARPin® molecules were successfully conjugated to the DGN549 payload
- DARPin® DGN549 conjugates bind to EGFR expressing cell lines with high affinity

DDC	DDR	EC_{50} nM	Monomer	Free drug	Yield
PSC099-DGN549	1.5	2.5	>95%	<1%	75%
PSC106-DGN549	1.7	2.6	>95%	<1%	70%
PSC108-DGN549	2.2	NA	>95%	<1%	40%

DDR: Drug to DARPin® molecule ratio

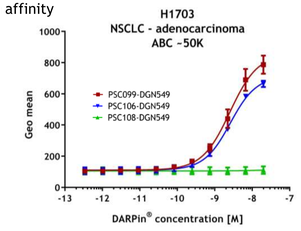

DARPin® drug conjugates have potent *in vitro* cytotoxicity against cell lines with a range of EGFR expression

- The *in vitro* potency of the EGFR-targeting DDCs was evaluated in a panel of cell lines expressing EGFR

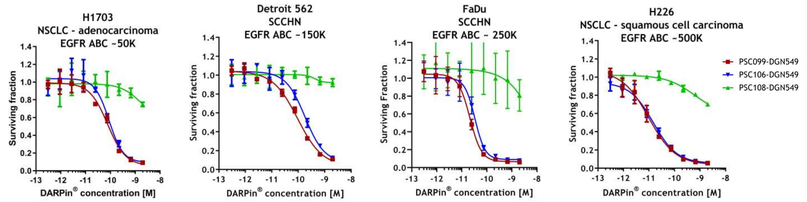

- The DARPin® DGN549 conjugates displayed pM potency in cell lines ranging in cell surface expression of EGFR from 50K to 500K antibodies bound per cell (ABC)

DARPin® drug conjugates are stable in circulation

- The pharmacokinetic (PK) profiles of the EGFR-targeting DARPin® drug conjugates were evaluated in CD-1 mice

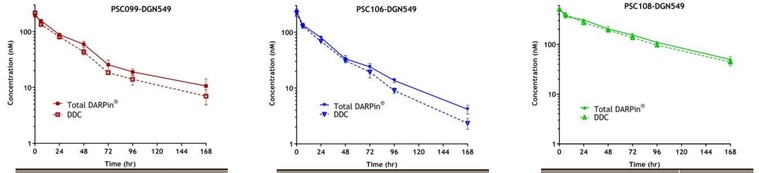

Molecule		Half-life (hr)
PSC099-DGN549	Total DARPin®	42
	DDC	38

Molecule		Half-life (hr)
PSC106-DGN549	Total DARPin®	33
	DDC	28

Molecule		Half-life (hr)
PSC108-DGN549	Total DARPin®	55
	DDC	52

- The PK profiles of intact DDCs and total DARPin® are similar demonstrating that the molecules are stable in circulation
- The non-targeting DDCs showed a terminal half-life of around 50 hrs. Murine cross-reactive EGFR DDCs showed half-lives of 28-38 hrs, indicating reasonable pharmacokinetic behavior in mice.

EGFR DARPin® drug conjugates demonstrate potent and antigen-specific anti-tumor activity *in vivo*

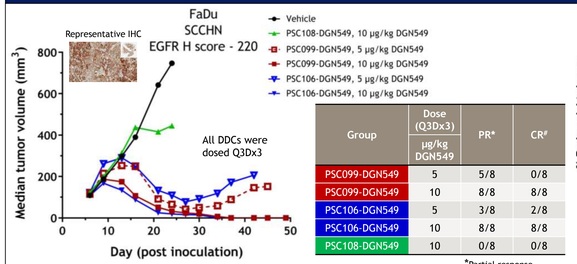

Group	Dose (Q3Dx3) µg/kg DGN549	PR*	CR#
PSC099-DGN549	5	5/8	0/8
PSC099-DGN549	10	8/8	8/8
PSC106-DGN549	5	3/8	2/8
PSC106-DGN549	10	8/8	8/8
PSC108-DGN549	10	0/8	0/8

*Partial response
#Complete response

The DDCs display dose dependent anti-tumor activity in an EGFR-expressing xenograft model

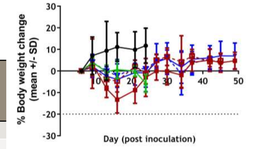

- The DDCs were well tolerated
- No mice lost >20% body weight and all body weight loss recovered over time

CONCLUSIONS

- EGFR DARPin® molecules bind to cells with high affinity and are internalized and trafficked to lysosomes
- DARPin® molecules display favorable conjugation properties (yield, % monomer, DDR, free drug) following conjugation to the DNA alkylator DGN549
- EGFR DARPin®-DGN549 conjugates have potent *in vitro* activity in a panel of cell lines expressing a range of EGFR levels
- The DARPin® drug conjugates are stable in circulation and have high anti-tumor activity in an EGFR expressing xenograft model
- DARPin® drug conjugates combine the potency of antibody drug conjugates and the modular DARPin® architecture to create designer therapeutics

Abstract

219

The potential benefit of lower drug-antibody ratio (DAR) on antibody-maytansinoid conjugate *in vivo* efficacy

Kerstin W. Sinkevicius, Leanne Lanieri, Jenny Lee, Steven Boulé, Nicholas C. Yoder, Stuart W. Hicks, Jan Pinkas, Jose F. Ponte, Richard J. Gregory

ImmunoGen, Inc, Waltham MA, USA

INTRODUCTION

- The majority of antibody-drug conjugates (ADCs) with maytansinoid payloads in development target a drug-antibody ratio (DAR) of 3.5, but lowering the DAR to 2.0 may be advantageous for some targets, like those with a sizable normal tissue antigen sink
- Since ADC tolerability is determined by the payload concentration, lower DAR ADCs can be dosed at a higher antibody (Ab) concentration, resulting in an increased conjugate exposure which may improve efficacy by saturating target-mediated drug disposition (TMDD) and increasing tumor penetration
- To investigate this hypothesis, the *in vivo* efficacy of standard (3.5) and lower (2.0) DAR antibody-maytansinoid conjugates were compared in xenograft models in which target expression was confined to the tumors or expressed in both the tumors and normal murine tissues using a cross-reactive system
- The DAR should be optimized for each target since the exposure advantage of lower DAR ADCs must outweigh their lower potency

ADC optimization for each target

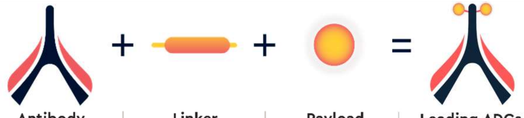

Antibody
- High specificity
- Optimal affinity
- Efficient internalization
- Low clearance
- Low immunogenicity
- Good tumor penetration

Linker
- Stable in circulation
- Efficient cleavage in tumor cells

Payload
- Highly potent
- Tumor cells susceptible to payload mechanism of action (MOA)
- Optimal drug-to-antibody ratio (DAR)
- High bystander killing

Leading ADCs

Methods

Efficacy studies: Tumor-bearing Nude or SCID mice were treated with anti-human ADCs or anti-mouse/human folate receptor α (FR)[1] maytansinoid payload (sSPDB-DM4 (solid lines) or DM21[2] (dashed lines) conjugated via lysines unless cysteine site-specific conjugation is specifically mentioned) ADCs. Tumor volume was calculated by the formula (LxWxH)/2. Activity was represented as tumor growth inhibition (%T/C), partial regressions (PR), and complete regressions (CR).

PK studies: SCID mice were dosed with a single intravenous injection of radiolabeled anti-mu/hu-FR. At time points ranging from 0.5 to 168 hours, plasma was collected for pharmacokinetic analysis based on the measured radioactivity.

Lower DAR ADCs are as efficacious as standard DAR ADCs in xenograft models in which tumors are the only source of target

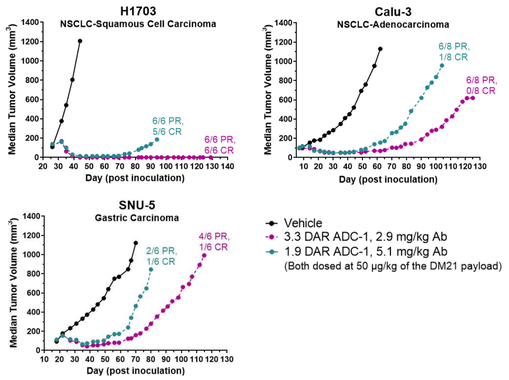

- Lysine-conjugated lower (1.9) and standard (3.3) DAR ADCs have comparable anti-tumor activity when dosed by the DM21 payload concentration
- Although the standard DAR ADCs are slightly more efficacious in these models, the benefit of lower DAR conjugates on saturating TMDD cannot be determined because the antibody in the ADC does not cross-react with the mouse target antigen expressed on normal tissues

Characterization of a cross-reactive system

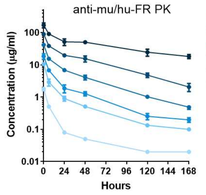

- A cross-reactive antibody was developed that utilizes a chimeric anti-murine folate receptor α (FR) antibody that binds with similar affinity to mouse and human FR
- Anti-mu/hu-FR mouse PK becomes linear at higher doses, most likely due to TMDD saturation*

*The mouse FR normal tissue sink is quite large compared to humans, in which PK linearity and TMDD saturation occurs at a lower dose

Lower DAR ADCs that can bind target expressed in normal tissues show improved efficacy in xenograft models

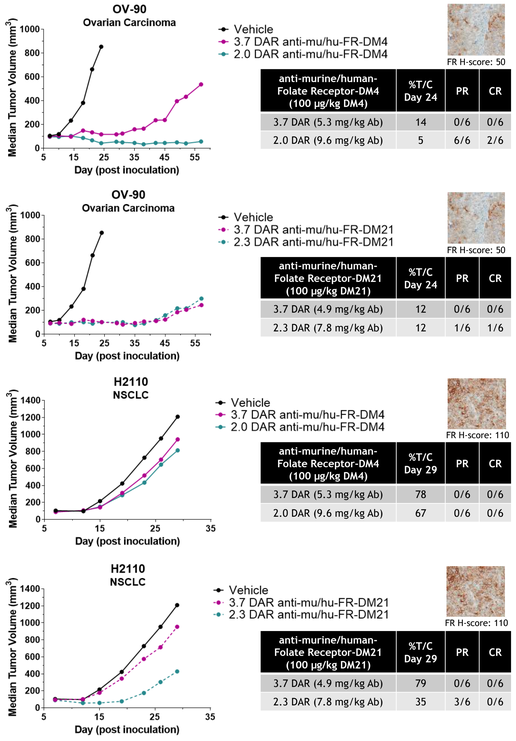

anti-murine/human-Folate Receptor-DM4 (100 µg/kg DM4)	%T/C Day 24	PR	CR
3.7 DAR (5.3 mg/kg Ab)	14	0/6	0/6
2.0 DAR (9.6 mg/kg Ab)	5	6/6	2/6

anti-murine/human-Folate Receptor-DM21 (100 µg/kg DM21)	%T/C Day 24	PR	CR
3.7 DAR (4.9 mg/kg Ab)	12	0/6	0/6
2.3 DAR (7.8 mg/kg Ab)	12	1/6	1/6

anti-murine/human-Folate Receptor-DM4 (100 µg/kg DM4)	%T/C Day 29	PR	CR
3.7 DAR (5.3 mg/kg Ab)	78	0/6	0/6
2.0 DAR (9.6 mg/kg Ab)	67	0/6	0/6

anti-murine/human-Folate Receptor-DM21 (100 µg/kg DM21)	%T/C Day 29	PR	CR
3.7 DAR (4.9 mg/kg Ab)	79	0/6	0/6
2.3 DAR (7.8 mg/kg Ab)	35	3/6	0/6

- This cross-reactive system demonstrates the potential benefit of lower DAR conjugates on saturating TMDD and improving efficacy

Site-specific conjugation may improve the efficacy of lower DAR ADCs

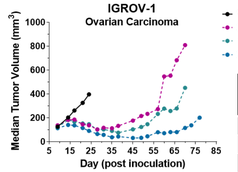

Vehicle
3.4 DAR anti-mu/hu-FR-DM21
1.9 DAR anti-mu/hu-FR-DM21
2.0 DAR anti-mu/hu-FR-C442-DM21


FR H-score: 165

anti-mu/hu-FR ADC Payload	DAR	DM21 Dose (µg/kg DM21)	Ab Dose (mg/kg)	PR	CR
Lysine-DM21	3.4	100	5.5	2/8	0/8
Lysine-DM21	1.9	100	9.6	2/8	0/8
C442-DM21*	2.0	100	9.6	5/8	0/8

*site-specific conjugation via two engineered cysteines in the Ab (CysMab)

- While lysine-conjugated lower (1.9) and standard (3.4) DAR ADCs have comparable anti-tumor activity in the cross-reactive system, the site-specific CysMab lower DAR (2.0) ADC is more active in this model

CONCLUSIONS

- Lowering the DAR of maytansinoid conjugates is one way to enhance ADC exposure, which may improve efficacy by saturating TMDD and increasing tumor penetration for some targets
- In murine models in which the tumor is the only source of target, lower and standard DAR ADCs have similar anti-tumor activity in xenograft models, but these results likely underestimate the potential efficacy improvements of lower DAR ADCs with targets with substantial TMDD
- In a cross-reactive system, where the ADC can also bind to target in normal tissues, lower DAR anti-murine/human-folate receptor maytansinoid conjugates are as or more efficacious than standard DAR conjugates when dosed at matched payload concentrations in xenograft models
- Preliminary results suggest that lower DAR site-specific CysMab conjugates may be more efficacious than lower DAR lysine linked conjugates in the cross-reactive system, demonstrating that conjugates with a homogeneous DAR may be advantageous for some models and targets

References:
- [1]AACR 2019 Abstract #229
- [2]AACR 2017 Abstract #2186

Abstract

Antibody-drug conjugates (ADCs) of a new class of *N*-10 amino-linked DNA-alkylating indolino-benzodiazepines (IGNs)

224

Michael L. Miller, Emily E. Reid, Katie E. Archer, Luke Harris, Erin K. Maloney, Laura M. Bartle, Olga Ab, Alan J. Wilhelm, Yulius Setiady, Jose F. Ponte, Rajeeva Singh, Thomas A. Keating, and Ravi V.J. Chari, ImmunoGen, Inc., Waltham, MA

INTRODUCTION

A novel class of DNA interacting payloads based on the highly potent DNA alkylating indolino-benzodiazepine (termed IGN) dimer have been prepared through the incorporation of a self-immolative peptide linker attached at the N-10 amine of the imine-reduced IGN monomer subunit.

- Objective – Synthesis of potent N-10 linked IGNs suitable for conjugation and incorporation into ADCs.
  - Compare the *in vitro* cytotoxicity of these N-10 linked IGN ADCs and their main catabolites in cancer cell lines with various levels of target-antigen expression.
  - Compare the *in vitro* bystander killing of the IGN ADCs.
  - Compare the interaction of the IGN catabolites with DNA.
  - Identify IGN ADCs which demonstrate a wide range of potency and tolerability to target cells/tumors with varying antigen expression levels.

Design Concept of the N-10 Linked IGNs

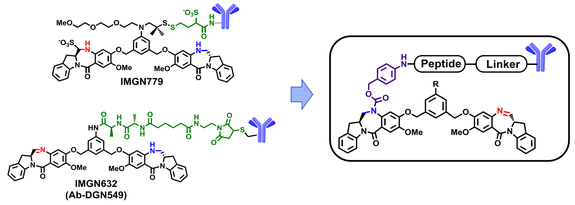

- IMGN779 and IMGN632 are clinical stage DNA alkylating IGN ADCs which were found to demonstrate an improved therapeutic index (TI) compared with those of DNA crosslinking IGN ADCs.
- A series of IGNs linked at the N-10 position using a *p*-aminobenzoyl (PAB) group with various peptide and linker motifs were prepared and PAB-Ala-Val-adipate was identified as a preferred linking group.
- Structure-Activity Relationship (SAR) studies focusing on modification of the spacer group linking the monomer subunits of the IGN dimer were conducted in an effort to improve the overall therapeutic index.

In Vitro Potency of IGN ADCs and Main Catabolites

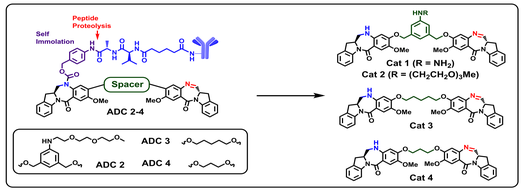

ADC	Cell Line	Indication	ABC# (x1000)	IC50 (pM) DGN549	ADC 2	ADC 3	ADC 4
Anti-FRα	KB	Cervical	3,000	4	20	30	100
Anti-EGFR	HSC2	Head/Neck	1,100	1	6	6	300
	KB	Cervical	158	6	40	40	3,000
	H2110	NSCLC	26	40	100	400	>10,000
				Cat 1	Cat 2	Cat 3	Cat 4
IGN Catabolite	KB	Cervical		8	20	20	200
	Namalwa	Lymphoma		2	3	3	30

- Modification of the IGN spacer led to ADCs that demonstrated a desirable range of *in vitro* potency which correlated with antigen expression, catabolite potency and tolerability.

IGN ADCs Demonstrate Potent Bystander Activity

- Total cell viability, which represents the capacity of an ADC to kill tumors with heterogenous expression through the direct killing of antigen positive cells, was measured on a mixed cell population*.
- All IGN ADCs demonstrated potent bystander activity indicating efficient catabolite formation and killing of antigen negative cells.

Anti-EFGR	Controls, IC50 (pM) Namalwa	MDA-MB-468	Bystander (pM) Total Cell Viability*
ADC 1	1	3	13
ADC 2	3	10	13
ADC 3	2	23	33
ADC 4	6	170	270

*MDA-MB-468 cells (1,000 cells/well) were mixed with Namalwa cells (500 cells/well) in U-bottom, low adherent wells and potency measured giving a readout of total cell viability.

IGN Catabolite Interaction with DNA

- DNA binding of IGN catabolite was measured against a reference IGN in a competitive inhibition assay using a hairpin oligonucleotide.
- A correlation of DNA binding with *in vitro* potency was observed.
- The use of an aromatic spacer appears to enhance DNA binding.

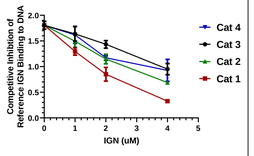

Adduct of IGN-biotin with Digoxigenin-46mer hairpin oligonucleotide (ELISA Absorbance)

ADC 4 and ADC 3 are Highly Active in Models with High and Medium Antigen Levels Respectively

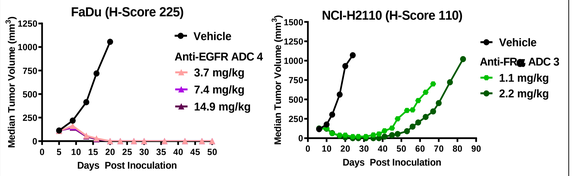

ADC	IGN Dose µg/kg	Ab Dose mg/kg	T/C (%) Day 20	PR	CR	Result
Anti-EGFR ADC 4 (FaDu, SCCHN)	80	3.7	0	6/6	6/6	Highly Active
	160	7.4	0	6/6	6/6	Highly Active
	320	14.9	0	6/6	6/6	Highly Active
Anti-FRα ADC 3 (NCI-H2110, NSCLC)	25	1.1	2	5/6	3/6	Highly Active
	50	2.2	0	6/6	6/6	Highly Active

SCID mice bearing FaDu (~100 mm3, day 5) or H2110 xenografts (~100 mm3, day 7) received a single IV injection.

- All IGN ADCs were dosed *in vivo* at consistent fractions of their respective MTD across all targets and models shown.
- All doses were well tolerated in mice.
- Anti-EGFR ADC 4 showed potent *in vivo* antitumor activity at low doses against a SCCHN xenograft model with high EGFR expression.
- Anti-FRα ADC 3 showed potent *in vivo* antitumor activity at low doses against a NSCLC xenograft model with medium FRα expression.

Anti-FRα ADC 2 is Highly Active Against the Low Antigen Expressing OV90 Ovarian Xenograft Model

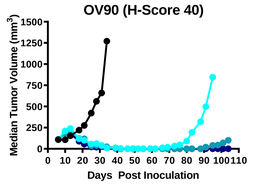

ADC	IGN Dose µg/kg	Ab Dose mg/kg	T/C (%) Day 42	PR	CR	Result
Anti-FRα ADC 2 (Ovarian)	15	0.7	6	6/6	6/6	Highly Active
	30	1.4	5	6/6	4/6	Highly Active
	60	2.7	4	6/6	5/6	Highly Active

Anti-FRα ADC 2 was Gln-Leu dipeptide for this experiment. SCID mice bearing OV-90 xenografts (~100 mm3) received a single IV injection of ADC on day 11.

- Anti-FRα ADC 2 shows *in vivo* anti-tumor activity at doses well below the MTD against an ovarian tumor xenograft model which expresses low heterogeneous FRα expression.

CONCLUSIONS

- A novel class of DNA-alkylating IGN dimer payloads has been prepared by incorporating a self-immolative peptide linker at the N-10 amine of an imine-reduced IGN monomer subunit.
- Modification of the central IGN Spacer led to IGN ADCs that showed a range of *in vitro* potency across cell lines with varying antigen levels which correlated with the catabolite potency, bystander activity, DNA interaction and tolerability.
- DNA-alkylating IGN ADCs demonstrated potent antigen-specific antitumor activity in tumor models possessing varying levels of antigen expression at doses well below the MTD.

American Association for Cancer Research, Annual Meeting 2019, March 29 – April 3, 2019, Atlanta, GA.

Utilizing a mouse cross-reactive model system to better understand antibody-drug conjugate pharmacokinetics, biodistribution, and efficacy

Abstract 229

Leanne Lanieri, Rassol Laleau, Bahar Matin, Luke Harris, Paulin Salomon, Jenny Lee, Steve Boulé, Michael Miller, Nicholas C. Yoder, Yulius Setiady, Neeraj Kohli, Thomas A. Keating, Jose F. Ponte, Jan Pinkas and Richard J. Gregory

INTRODUCTION

Antibody-drug conjugates (ADCs) are designed to deliver a potent cytotoxic payload directly to tumors, thus limiting exposure in normal tissues. However, target antigen expression on normal tissues can lead to lower systemic ADC exposures, resulting in sub-efficacious concentrations at the tumor site as well as heterogeneous distribution within tumors. Traditional preclinical efficacy studies performed in rodent models using non-cross-reactive ADCs have had limited use in improving our understanding of the factors that influence ADC dose and activity. To examine relationships between variables that could impact ADC efficacy, we generated a cross-reactive chimeric anti-murine folate receptor α (FRα) antibody (designated FR1-12) that binds both mouse and human FRα, and can be conjugated to either maytansinoid (DM) or indolinobenzodiazepine (IGN) payloads. This model system was predicted to have substantial target-mediated drug disposition (TMDD) due to normal tissue expression of FRα. Using these ADCs, we assessed the impact of xenograft antigen expression, ADC dose and drug-to-antibody ratio (DAR) on the PK, biodistribution, and efficacy of the FR1-12 ADC.

Methods

Antibody Generation: Rabbits were immunized with a mouse FRα expressing 300-19 cell line. The resulting antibody was chimerized to a mouse IgG2a (mulgG2a) backbone and designated rmFR1-12. Binding to mouse and human FRα was comparable. Data using a rmFR1-12-s-SPDB-DM4 ADC is presented here. Naked rmFR1-12 antibody was used in antibody dilution studies.

In Vivo Efficacy: KB-bearing SCID mice were treated with ADC and/or naked antibody. Tumor volume was calculated by the formula (LxWxH)/2. Activity was represented as %T/C, partial and complete regressions.

Biodistribution: KB-bearing SCID mice were given a single IV injection of radio-labeled ADC. At time points ranging from 0.5 to 72 hours, a selection of tissues were collected, homogenized and payload concentration in the tissues was determined based on the measured radioactivity. Plasma was also collected for pharmacokinetic analysis based on the measured radioactivity.

Cross-Reactive Model System

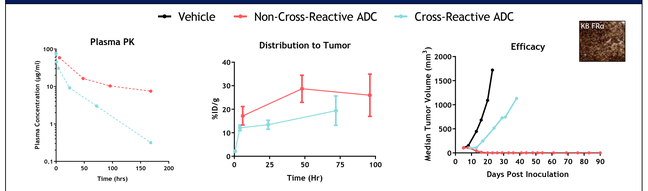

- Normal tissue antigen expression in our cross-reactive model system leads to significant PK encumbrance, less ADC delivery to the tumor and a decrease in anti-tumor activity in KB xenografts with high FRα expression.

The Impact of Dose on PK, Biodistribution and Efficacy

PK and Efficacy are Enhanced as the Dose Increases

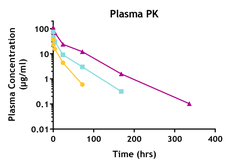

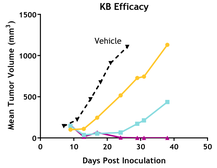

Dose	AUC_{ALL} (pmole/g)
ADC 2.5 mg/kg	9739
ADC 5 mg/kg	23576
Fold Difference vs 2.5 mg/kg	2.4
ADC 10 mg/kg	49561
Fold Difference vs 2.5 mg/kg	5.1

Group	T/C (%)	PR	CR	Result
ADC 2.5 mg/kg	17	0/3	0/3	Active
ADC 5 mg/kg	5	3/3	1/3	Highly Active
ADC 10 mg/kg	5	3/3	3/3	Highly Active

As ADC dose increases:
- ↑ C_{max}
- ↓ clearance
- ↑ time in circulation
- ↑ exposure

- Direct correlation between dose and activity

Biodistribution to Select Tissue and Tumor

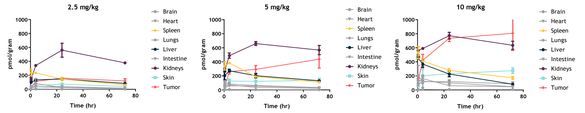

Dose	AUC_{ALL} (pmole/g)				
	Spleen	Liver	Kidneys	Skin	Tumor
ADC 2.5 mg/kg	9696	8806	32427	4204	9739
ADC 5 mg/kg	14178	13583	42266	8981	23576
Fold Difference vs 2.5 mg/kg	1.5	1.5	1.3	2.1	2.4
ADC 10 mg/kg	19429	14811	49413	16948	49561
Fold Difference vs 2.5 mg/kg	2.0	1.7	1.5	4.0	5.1

- Local exposure increased with ADC dose
- Mouse kidney has high FRα expression
- Kinetics of delivery is different for most normal tissue vs tumor
- As TMDD becomes saturated, more ADC available to tumor

Impact of DAR on PK, Biodistribution and Efficacy

ADC PK Is Enhanced by Increasing Addition of Naked Antibody

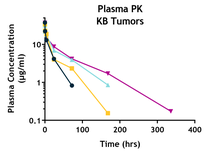

Group	C_{Max} (µg/ml)	T_{Last} (hr)	$AUC_{0-\infty}$ (hr*µg/ml)
ADC 2.5 mg/kg	37.6	72	389
ADC 2.5 mg/kg + Ab 2.5 mg/kg	34.1	168	593
ADC 2.5 mg/kg + Ab 10 mg/kg	31.8	168	874
ADC 2.5 mg/kg + Ab 25 mg/kg	37.3	336	1084

Addition of naked Ab:
- Has no impact on ADC C_{max}
- ↑ Ab C_{max} with ↑ dose of naked Ab
- ↑ time ADC is in circulation
- ↑ exposure

ADC Biodistribution To Select Tissue and Tumor

No FRα Organs

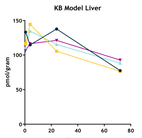

Group	AUC_{All} (hr*nmole/g)
ADC 2.5 mg/kg	8125
ADC 2.5 mg/kg + Ab 2.5 mg/kg	7328
ADC 2.5 mg/kg + Ab 10 mg/kg	7818
ADC 2.5 mg/kg + Ab 25 mg/kg	7904

No impact on delivery

High FRα Organs

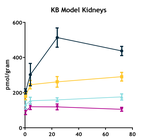

Group	AUC_{All} (hr*nmole/g)
ADC 2.5 mg/kg	31872
ADC 2.5 mg/kg + Ab 2.5 mg/kg	19066
ADC 2.5 mg/kg + Ab 10 mg/kg	11658
ADC 2.5 mg/kg + Ab 25 mg/kg	8128

Significant ↓ on delivery

High FRα Tumor

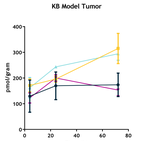

Group	AUC_{All} (hr*nmole/g)
ADC 2.5 mg/kg	11,241
ADC 2.5 mg/kg + Ab 2.5 mg/kg	15,932
ADC 2.5 mg/kg + Ab 10 mg/kg	16,965
ADC 2.5 mg/kg + Ab 25 mg/kg	11,710

Modest ↑ at 2.5 and 10 mg/kg
No impact at 25 mg/kg

Addition of Antibody Can Increase ADC Efficacy

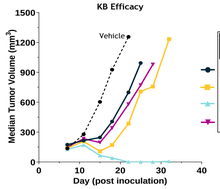

Group	T/C (%)	PR	CR	Result
ADC 2.5 mg/kg	56	1/6	0/6	Inactive
ADC 2.5 mg/kg + Ab 2.5 mg/kg	31	0/6	0/6	Active
ADC 2.5 mg/kg + Ab 10 mg/kg	0	6/6	4/6	Highly Active
ADC 2.5 mg/kg + Ab 25 mg/kg	46	0/6	0/6	Inactive

PBPK Model Construction

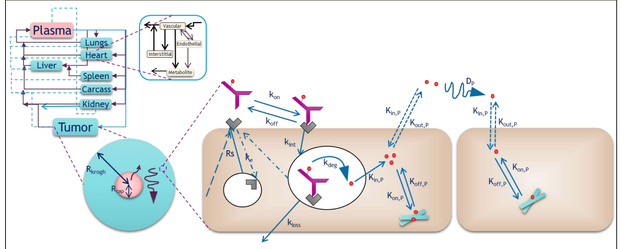

- A mechanistic tumor penetration model incorporated into a physiologically based pharmacokinetics model has been generated to analyze the rm-FR1-12-ADC experiment results and quantify ADC and payload tumor penetration.

Adapted from Cilliers et al., 2016, AAPSJ, 18(5); 1117-30

CONCLUSIONS

- TMDD significantly impacts ADC delivery and efficacy
- Using labeled payload allows us to assess ADC distribution on multiple levels
  - Systemic and local exposure increases with dose
  - Kinetics of delivery is different between tumor and most normal tissue
  - As TMDD becomes saturated, more ADC is available to reach the tumor
  - There is a direct correlation between ADC dose and activity
- Decreasing effective DAR via naked antibody dilution impacts PK, biodistribution and efficacy
- Distribution of ADC across the tumor is just as important as the amount of ADC that reaches the tumor

Abstract

Antibody-drug conjugates (ADCs) with indolinobenzodiazepine dimer (IGN) payloads: DNA-binding mechanism of IGN catabolites in target cancer cells

230

Rajeeva Singh, Luke Harris, Paulin L. Salomon, Emily E. Reid, Michael L. Miller, Ravi V. J. Chari, and Thomas A. Keating
ImmunoGen, Inc., Waltham, MA

INTRODUCTION

ImmunoGen's IMGN779 and IMGN632 ADCs employ DNA-alkylating, mono-imine indolinobenzodiazepine dimer (IGN) payloads, linked via disulfide or peptide linker, respectively

In contrast, ADCs of pyrrolobenzodiazepine dimer (PBD) payloads, talirine and tesirine, employ a DNA cross-linking di-imine moiety

Goals of this investigation:

- To understand the DNA-binding mechanism of IGN payloads
- Develop sensitive assays to measure IGN-DNA binding of mono-imine versus di-imine payloads at IC_{50} concentrations in cells
- DNA repair of IGN-DNA adducts probed using nucleases as models

Methods

- Duplex and hairpin oligonucleotides of high melting temperature custom synthesized with biotin, digoxigenin, or Alexa label
- Synthetically derived IGN1-biotin (mono-imine), IGN2-biotin (di-imine), and IGN3-biotin (di-amine) used as model IGN catabolites
- ELISA: Anti-DNA antibody (MAB030; EMD Millipore) for DNA-bound biotin-IGN assay. Biotin-IGN released upon DNA cleavage by added nuclease was assayed by digoxigenin-oligonucleotide reaction, streptavidin coat/anti-digoxigenin Ab-HRP detection

Structures of IGNs, PBDs, and Oligonucleotide

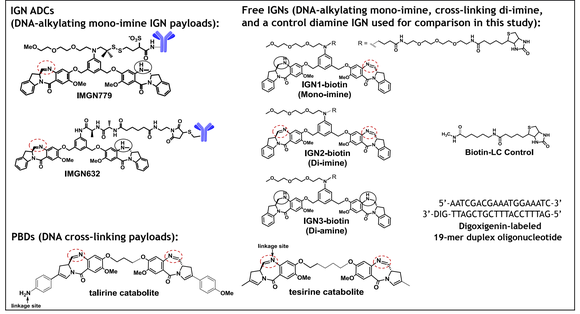

IGN Binding to DNA in Cancer Cells

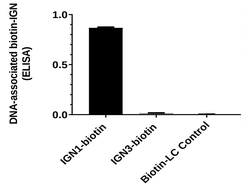

HSC-2 cells were treated with 0.5 uM IGN1-biotin or IGN3-biotin, or 1 uM biotin-LC control for 1 day

Genomic DNA was isolated

ELISA using anti-DNA antibody for capture and streptavidin-HRP conjugate for detection

- Mono-imine IGN (IGN1-biotin) forms stable covalent adduct with DNA in cells, but not di-amine IGN (IGN3-biotin)

Time Course of IGN-DNA Adduct Formation in Cells

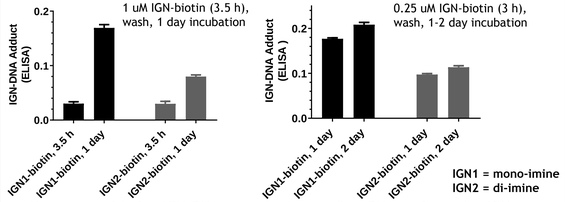

- Mono- and di-imine IGN-DNA adducts: 1 day > 3 h. DNA available for IGN reaction presumably during replication and transcription
- Stable DNA adducts observed at 2 days for both IGN1-biotin and IGN2-biotin
- DNA adduct IGN1 > IGN2 (presumably better cellular and nuclear permeability)

In Vitro Cytotoxicity of IGNs

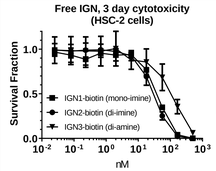

Free IGN	IC_{50} (nM), 3 day
IGN1-biotin	30
IGN2-biotin	35
IGN3-biotin	100

IGN ADC (FRα)	IC_{50} (pM), 5 day (KB cells)[1]
IGN1	20
IGN2	15
IGN3	not done

Potency: IGN1 ≈ IGN2 > IGN3

- Mono- and di-imine IGNs (IGN1, IGN2) are more potent than di-amine IGN (IGN3). Cytotoxicities of both free IGNs and IGN ADCs correlate with DNA binding

Dissociation of IGN-DNA Adduct Upon DNA Cleavage

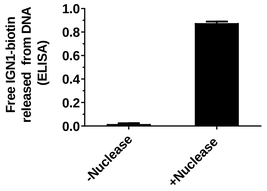

IGN1-biotin adduct with 46-mer hairpin oligonucleotide → Treatment with DNase I + Micrococcal nuclease, 37 °C

ELISA detection of released biotin-IGN1 using digoxigenin-labeled 19-mer duplex oligonucleotide

- Mono-imine IGN forms highly stable DNA adduct: No dissociation without added nuclease
- DNAse I efficient for DNA cleavage and IGN-DNA adduct dissociation, 37 °C (physiological conditions). Adduct reversal also observed with other nucleases

Mono- and Di-imine IGN-DNA Adducts: DNA Cleavage

HSC-2 cells: 0.5 uM IGN1-biotin (mono-imine), or IGN2-biotin (di-imine), 1 day. Genomic DNA isolated.

DNA incorporation of IGN1 about 3-fold more than IGN2 (anti-DNA antibody ELISA), presumably due to better cellular/nuclear permeability of IGN1-biotin

IGN release from adduct by nuclease treatment:

Mono- and di-imine IGN-DNA adducts normalized for equal level (based on anti-DNA antibody ELISA). Treated with DNase I, 37 °C.

Released free IGN-biotin drug measured by digoxigenin-oligonucleotide reaction ELISA (using free IGN1-biotin and IGN2-biotin standards)

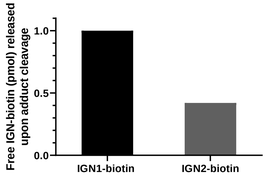

➢ Ratio of released IGN1-biotin (mono-imine)/IGN2-biotin (di-imine) = 2.4/1

- DNA cleavage by DNase results in about 2-fold greater release of free IGN1 (mono-imine) than IGN2 (di-imine)
- IGN2 (di-imine) could be partly cross-linked to genomic DNA

Competition by Inosine Oligonucleotide to the Binding of Guanine Oligonucleotide with IGN

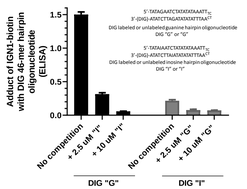

Binding of IGN1-biotin (mono-imine) to Digoxigenin (DIG)-labeled 46-mer Guanine (DIG "G") or Inosine (DIG "I") containing hairpin oligonucleotide (12 nM each):

Competition with unlabeled Inosine ("I") or Guanine ("G") containing hairpin oligonucleotide

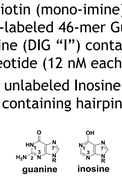

- Adduct of mono-imine IGN with guanine containing hairpin more stable than with inosine containing hairpin (under ELISA conditions with multiple washes)
- Inosine hairpin kinetically competes with the guanine hairpin oligonucleotide

Mechanism of IGN-DNA Adduct Formation

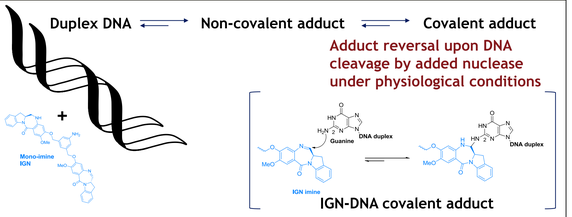

CONCLUSIONS

- ImmunoGen's DNA-alkylating mono-imine IGN payload generates highly stable IGN-DNA adduct in cells
- Cleavage of IGN-DNA adduct by nuclease at 37 °C leads to IGN dissociation, indicating potential DNA repair by endonucleases
- Upon nuclease treatment, more drug released from DNA adduct of alkylating mono-imine than cross-linking di-imine payload

References:

1. Miller, M. L., et al., *Mol. Cancer Ther.* 2016, 15, 1870-1878
2. Miller, M. L., et al., *Mol. Cancer Ther.* 2018, 17, 650-660
3. Mantaj, J., et al., *PLoS One*, 2016, DOI:10.1371/journal.pone.0152303

American Association for Cancer Research (AACR) Annual Meeting, March 29 - April 3, 2019, Atlanta, GA.

Abstract

Optimizing lysosomal activation of antibody-drug conjugates (ADCs) by incorporation of novel cleavable dipeptide linkers

231

Paulin L. Salomon, Luke Harris, Emily E. Reid, Erin K. Maloney, Alan J. Wilhelm, Michael L. Miller, Ravi V.J. Chari, Thomas A. Keating, Rajeeva Singh
ImmunoGen, Inc., Waltham, MA

INTRODUCTION

- Optimal linker for an ADC
  - ➢ Stable in circulation
  - ➢ Cleaved efficiently in lysosomes
- Dipeptide linker screening for lysosomal proteolysis
  - ➢ Fluorogenic leaving group, 7-amino-4-methylcoumarin (AMC) on dipeptides, convenient for proteolytic assay
- Selected dipeptide linkers incorporated into ADCs bearing a DNA-alkylating indolinobenzodiazepine (IGN) payload
  - ➢ Target cell processing, cytotoxic activity, in vivo efficacy, stability measured

Dipeptide linker ADC with IGN payload

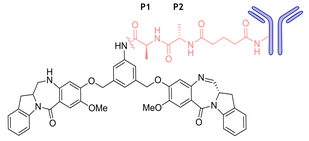

Fluorogenic dipeptide linker proteolysis screen

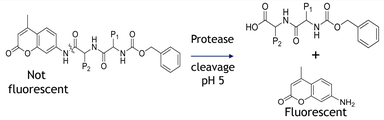

Incubated with cell lysate, purified Cathepsins (pH ~5), or plasma (pH 7.5); increase in fluorescence measured

Relative substrate cleavage score of Z-P2-P1-AMC peptides with cell lysate and purified Cathepsins

Peptide Sequence, P2-P1	YR	FR	VQ	VC	YM	LQ	VR	MT	FQ	TT	VT	AA	VM	LM	AN	GGR	dVdQ	VA	dAdA	FM
Cell Lysate	100	71	**63**	51	48	42	38	25	17	12	8	**7**	4	4	4	4	4	3	2	0
Cathepsin L	-	100	**60**	6	55	55	23	-	69	46	13	**0**	-	-	1	-	-	0	-	-
Cathepsin B	-	100	**87**	33	47	73	43	-	19	18	12	**4**	-	-	0	8	-	0	-	-
Cathepsin S	-	35	**16**	9	-	100	-	-	7	-	-	**2**	-	-	-	-	-	0	-	-
Cathepsin F	-	100	**28**	13	-	35	-	-	21	-	-	**3**	-	-	-	-	-	0	-	-

- 20 dipeptides were synthetized as AMC constructs and cleavage rates analyzed using different cell lysates and purified Cathepsins.
- Gln (Q) at P1 as an anilino-peptide showed a high level of activity and stability upon conjugation.

Short-term processing of ADCs in target cells

- Processing of dipeptide linked IGN ADCs in FRα cell lines (13 nM ADC, 2 h, wash, 4 h-1 day processing)
- Val-Gln linked ADCs generated greater amount of catabolites at earlier time points. Advantageous in lower ABC cell lines

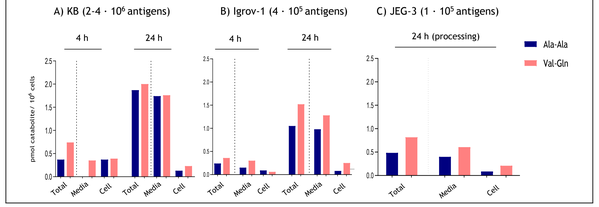

ADC processing in the presence of Bafilomycin A1

- Baf A1 inhibits ATP-pumps;
  - ➢ Lysosomal pH stays elevated, proteases are less active
- 1 day processing assay with and without co-incubation of Bafilomycin A1. Short-term processing is abolished
- Val-Gln linked ADC generates greater amount of catabolites than Ala-Ala dipeptide. Under limited lysosomal function, processing of Val-Gln is more efficient

HSC2, αEGFR (1 · 10⁶ antigens)

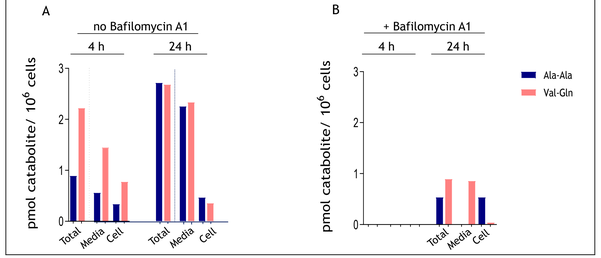

In vitro cytotoxicity of ADCs

- 5 day cytotoxicity assay in EGFR or FRα positive cell lines
- Cleavable dipeptide linked ADCs are more active than ADCs with non-cleavable linker design
- Val-Gln linker shows similar or greater activity than Ala-Ala peptide linker

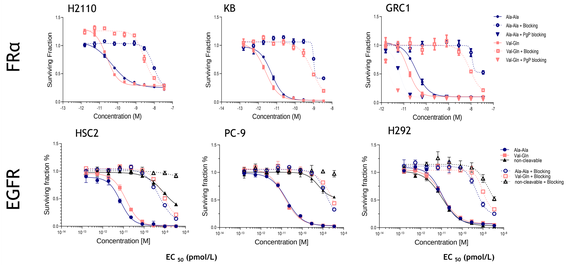

EC $_{50}$ (pmol/L)

αEGFR-ADC	HSC2	PC-9	SAS	H1975	H292	BxPC3
Val-Gln-IGN	14	13	4.7	99	12	39
Ala-Ala-IGN	7.5	17	6.1	93	11	45
non-cleavable-IGN	860	580	170	1100	11	38

EC $_{50}$ (pmol/L)

αFRα-ADC	Igrov-1	KB	H2110	T47D	OV-90	GRC1*
Val-Gln-IGN	18	3	50	20	30	20
Ala-Ala-IGN	9.3	5	200	30	30	40

* GRC1, positive for multidrug-resistant (MDR) PgP efflux pump

In vivo efficacy and tolerability of new linkers

- Efficacy of dipeptide linked ADCs were tested in a NCI-H2110 xenograft tumor model in mice
- All tested peptide sequences showed similar tolerability
- Both Val-Gln and Ala-Ala linked ADCs were highly active at 3 ug/kg drug dose, Val-Thr was active at that dose

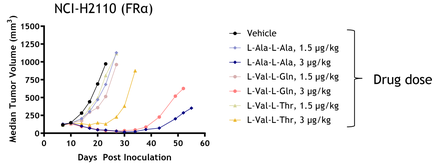

Threshold for cytotoxic activity

- Cell doubling within ~24 h, similar catabolite amounts above cytotoxic threshold generated for both linkers
- Lysosomal processing may not be rate limiting for activity

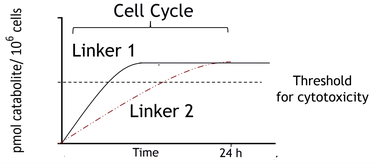

CONCLUSIONS

- Fluorogenic dipeptide screen identified several new linkers: Val-Gln, Leu-Gln, Tyr-Met, Val-Arg
- Lysosomal processing of ADCs showed greater amounts of released catabolites for Val-Gln over Ala-Ala linked ADCs at early time points and under limited lysosomal proteolysis with Bafilomycin A1
- Increased proteolysis did not result in better cytotoxicity. This may point to catabolite generation not being rate determining in this assay or catabolites reaching threshold limits for activity
- Low target antigen-expressing cell line or tumor could show advantage for Val-Gln linker due to increased processing
- In vivo, the lead dipeptide linker Val-Gln ADC was highly active at 3 µg/kg and tolerated at ~ 100 µg/kg drug dose

References:

1. Miller, M. L., et al. *Mol. Cancer Ther.* 2018,17, 650-660

2019 AACR Annual Meeting, March 29 - April 3, 2019, Atlanta, GA

LC-MS Based Catabolite Identification Study of an ADC with DM21-C, a Novel Maytansinoid Linker-Payload

Abstract 538

Janet Lau, Paulin L. Salomon, Kerstin Sinkevicius, Juliet Costoplus, Megan Fuller, Jenny Lee, Raymond Xu, Stuart Hicks, Ravi Chari, Wayne Widdison, Nicholas Yoder, Thomas Keating

ImmunoGen, Inc. 830 Winter Street, Waltham, MA 02451

INTRODUCTION

- Maytansinoid-based DM21-C is one of ImmunoGen's newest payloads benefiting from a peptidase/protease cleavable linker.[1,2]

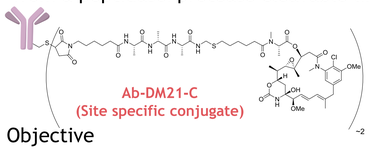

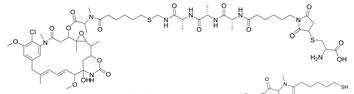

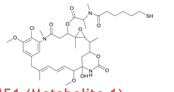

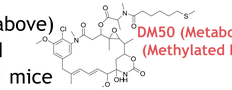

- Objective

- Conduct *in vitro* catabolism studies to identify the major catabolites generated when a DM21-C ADC was incubated with antigen-positive tumor cells. Several catabolites were predicted to be formed (shown as above)
- Determine the *in vivo* catabolites of DM21-C payload for the ADC in the plasma of non-tumor bearing CD-1 mice

Experimental Design and Methods

***In vitro* study with SNU-5 cell and media:**

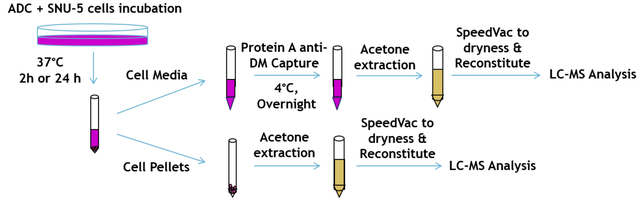

***In vivo* study with female CD-1 mice:** Different sub-groups of mice (n=3) were euthanized at 2h, 6h and 24h following the IV administration of ADC at 350 µg/kg DM21-C (35.6 mg/kg ADC) and cardiac puncture bleeds were performed. Blood from untreated mice (n=3) was also collected and analyzed as a control. Collected whole blood was processed to plasma using K_2 EDTA micro hematocrit plasma collection tubes after 5 µl of 0.5M NEM was added to cap free thiols. Catabolites were extracted with acetone and analyzed with LC-MS.

DM21-C Catabolites Identified with High Resolution MS

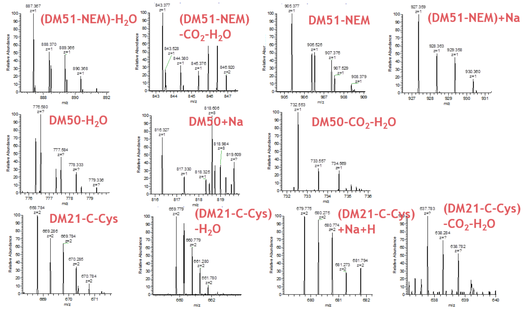

- DM51-NEM, DM50 and DM21-C-Cys related ions were identified with high confidence from the SNU-5 cell pellet with high resolution mass spec (Q Exactive) in the presence of complex background matrix.

Summary of *in vitro* and *in vivo* Catabolite ID Results

***In vitro* Catabolite ID with SNU-5 cell pellet and cell media:**

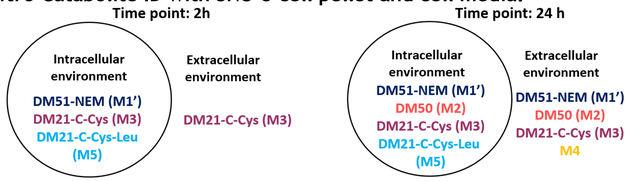

- Major catabolites M1 to M5 were identified with LC-MS from SNU-5 cell pellet or media upon incubation with DM21-C containing ADC for 2h or 24h.

***In vivo* Catabolite ID from mouse plasma:**

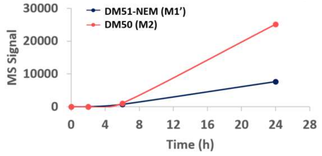

- Catabolite DM51-NEM (M1') and DM50 (M2) were identified with LC-MS at later time points (6 h and 24 h) at concentration <10 ng/mL, suggesting the mouse *in vivo* stability of DM21-C, as well as the high sensitivity of developed LC-MS method.

Proposed Catabolic Pathway from SNU-5 Cell *in vitro* Study

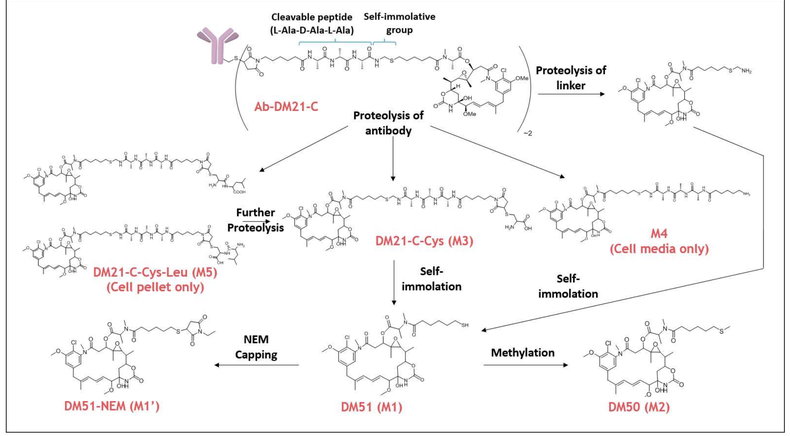

CONCLUSIONS

- Catabolites generated upon incubation of DM21-C bearing ADC with antigen-positive cancer cells were identified via LC-MS from both cell pellet and cell media. Self-immolation catabolite DM51, its methylated form DM50 and DM21-C-Cys were identified as major products. A catabolic pathway was proposed based on the *in vitro* study with SNU-5 cells using the optimized sample preparation and high resolution mass spec analysis.
- An *in vivo* study in non-tumor bearing mice showed that DM21-C containing ADCs are stable in circulation with only low concentrations of DM51 and DM50 detected at later time points.

References:

[1] Widdison, W. C. et al., *Bioconj. Chem.*: **2015**, *26*, 2261-2778.

[2] Costoplus, J. A. et al., Peptide-Cleavable Self-Immolative Maytansinoid Antibody Drug Conjugates Designed to Provide Improved Bystander Killing (manuscript in preparation)

Preclinical evaluation of DM21, a next-generation maytansinoid payload with a stable peptide linker

Abstract 3898

Wayne Deats, Wayne Widdison, Juliet Costoplus, Bahar Matin, Nicole McBrine, Laura Bartle, Olga Ab, Richard Gregory, and Jan Pinkas
ImmunoGen, Inc. 830 Winter Street, Waltham, MA, 02451

INTRODUCTION

- DM21 is a novel maytansinoid payload containing a tripeptide linker (L-Ala-D-Ala-L-Ala) designed to have increased cytotoxicity, bystander killing, efficacy and linker stability compared to sSPDB-DM4
- The platform (non-targeted) toxicity of this payload was evaluated by conjugating DM21 to lysine residues on the non-cynomolgus monkey cross-reactive antibody chKTI (a chimeric human IgG_1 anti-soybean trypsin inhibitor antibody)

Methods

Bystander Assay

- Antigen-negative Namalwa-Luciferase cells were incubated with increasing numbers of an antigen-positive cell line and exposed to 2 nM concentrations of either sSPDB-DM4 or DM21 conjugates for 5 days, and the percentage of surviving Namalwa-Luciferase cells was assessed at the end of the exposure

Toxicity Study

- Naïve cynomolgus monkeys were administered chKTI-DM21-L or vehicle as a single 10-minute IV infusion
- Toxicity was determined based upon clinical observations, body weights, ophthalmic examinations, and clinical and anatomic pathology; plasma and serum samples were collected to evaluate the toxicokinetic profile

Bystander Assay

- The DM21 conjugate resulted in appreciably greater bystander killing of antigen negative Namalwa-Luciferase cells, compared to the sSPDB-DM4 conjugate

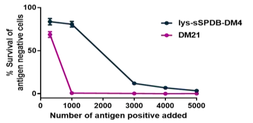

Toxicity Study Design

- Animals were randomized and assigned to the following study groups

Group	Dose Level (DAR 3.46)		N	
	Ab	DM21	Day 5 Necropsy	Day 29 Necropsy
1	0 mg/kg	0 µg/kg	3M	2M
2	11 mg/kg	204 µg/kg	3M	2M
3	22 mg/kg	408 µg/kg	3M	2M

Clinical Observations and Body Weight

- All doses were well tolerated
- No effect on BW; clinical observations included reddened/darkened skin and scabbing (all dose groups) and soft/liquid feces (22 mg/kg)

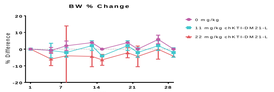

Pharmacokinetics

- chKTI-DM21-L has dose-proportional exposure and linear PK
- ADC and TAb followed a biphasic PK curve consistent through 336 hours after dosing, suggesting that the administered conjugates were stable
- TAb divergence from the ADC concentration-time curves resulted in TAb's longer half-life and higher exposure

Dose Group		T1/2 (hr)	AUC_{0-672} (hr*µg/mL)	C_{max} (µg/mL)
ADC	11 mg/kg	188 ± 28.3	34300 ± 236	316 ± 27.6
	22 mg/kg	178 ± 29.3	65700 ± 8740	689 ± 35.7
TAb	11 mg/kg	248 ± 79.8	32200 ± 4020	303 ± 51.2
	22 mg/kg	252 ± 41.4	72100 ± 10900	672 ± 44.2

Data shows mean ±SD of parameter values.

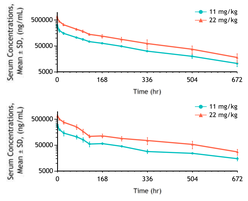

Clinical Pathology

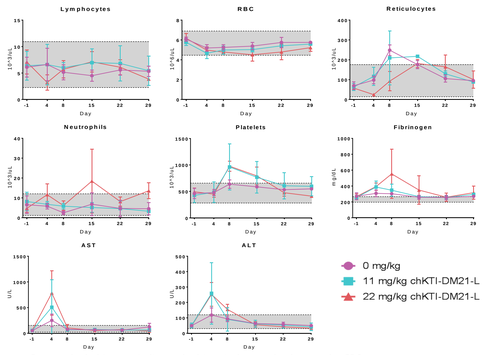

Ranges shaded in grey indicate the historical control values at the CRO

- chKTI-DM21-L related clinical pathology effects were noted for WBC and RBC parameters
- Elevations in platelets and fibrinogen correlated with skin observations
- Elevations in liver enzymes were noted, however there were no correlating histopathology findings

Organ Weights

- Non-adverse decreased thymus weights at the terminal and recovery necropsies at 11 and 22 mg/kg
  - No microscopic correlates or effects on any other immunologic organs

	Terminal Necropsy			Recovery Necropsy		
Dose Group	0 mg/kg	11 mg/kg	22 mg/kg	0 mg/kg	11 mg/kg	22 mg/kg
Mean	3.0367	2.5767	1.4700	3.3750	2.3300	1.6900
SD	1.5837	0.9215	0.7251	1.4779	1.5839	1.6546
N	3	3	3	2	2	2
% Difference	--	-15%	-52%	--	-31%	-50%

Anatomic Pathology

- Epithelial degeneration was noted in the large intestine (cecum, colon, and rectum) at the terminal necropsy at 22 mg/kg
  - Characterized by a loss of epithelial cells and collapse of the mucosa, without associated inflammation or necrosis
  - These findings were not present at the recovery necropsy

	Terminal Necropsy			Recovery Necropsy		
Dose Group	0 mg/kg	11 mg/kg	22 mg/kg	0 mg/kg	11 mg/kg	22 mg/kg
Large intestine, cecum (examined)	3	3	3	2	2	2
Degeneration, epithelial, mild	--	--	1	--	--	--
Degeneration, epithelial, moderate	--	--	2	--	--	--
Large intestine, colon (examined)	3	3	3	2	2	2
Degeneration, epithelial, mild	--	--	1	--	--	--
Degeneration, epithelial, moderate	--	--	2	--	--	--
Large intestine, rectum (examined)	3	3	3	2	2	2
Degeneration, epithelial, mild	--	--	1	--	--	--

CONCLUSIONS

- DM21 has increased bystander killing as compared to sSPDB-DM4
- chKTI-DM21-L was well tolerated at doses up to and including 22 mg/kg (408 µg/kg DM21)
  - No adverse effects on body weights, clinical signs, or clinical pathology or organ weights
  - Histopathology findings noted in the 22 mg/kg group at the terminal necropsy were not present at the recovery necropsy
- Evaluation of PK data suggest that chKTI-DM21-L is a stable conjugate
- DM21 is an exciting next generation maytansinoid payload ready for preclinical development

American Association for Cancer Research, Annual Meeting 2019, 29 March – 03 April 2019

Abstract
4817

Preclinical Evaluation of a New, Non-Agonist ADC Targeting *MET*-Amplified Tumors with a Peptide-linked Maytansinoid

Katharine C. Lai, Min Li, Kathryn Selvitelli, Surina Sikka, Steven Boulé, L. Cristina Gavrilescu, Kerry Donahue, Stuart W. Hicks
ImmunoGen, Inc. Waltham, MA

INTRODUCTION

With cancer among the leading causes of death worldwide, the search for better, personalized treatments is imperative. Novel techniques such as next generation sequencing have identified many assayable genetic biomarkers associated with cancer in patient samples. The tyrosine kinase receptor cMet is one such biomarker that is upregulated in various solid tumors and associated with poor prognosis, disease progression and metastasis. While most patients with elevated cMet show increased levels through protein upregulation, a small population harbors gene amplification. These patients face worse outcomes which could be improved with therapies specifically targeting their *MET*-amplification. Antibody-drug conjugates (ADCs) are a modality designed to selectively deliver highly potent cytotoxic agents to tumors. cMet is an attractive target for ADCs which may address the unmet treatment need for patients with tumors harboring *MET* amplification.

Methods

Antibody discovery and design: As previously described, we identified and humanized an antibody (Ab) with minimal agonism from a panel of hybridoma-derived Abs, hucMet27. Introducing an additional disulfide in the hinge region while maintaining the IgG1 isotype further reduced agonism in assays described below.

In vitro signaling assays: To determine potential agonist activity of anti-cMet Abs via cell proliferation, NCI-H441 cells were plated in serum-free media (SFM) overnight before treatment with varying concentrations of test article in triplicate. Plates were incubated for 4 days prior to WST-8 treatment and analysis. To assess cMet activation, phosphorylation of down-stream markers AKT and ERK were measured by ELISA; NCI-H441 cells were plated in SFM overnight before treatment with 10 ug/mL test article in triplicate. After 30 mins cells were lysed and phosphorylation measured by ELISA.

Binding: To measure binding to both human and cyno cMet by ForteBio, his-tagged soluble recombinant human cMet or cyno cMet ECD protein (2.6- 30 nM) was incubated with anti-human Fc capture biosensors loaded with immobilized anti-cMet Ab at 10 nM. The kinetics of binding were determined using a 1:1 binding fit model. To assess binding to cancer cell lines and primary human/cyno hepatocytes, cell-based binding was carried out for 1 hour at 4ºC. Samples were washed twice with staining buffer, incubated with FITC goat anti-human IgG secondary Ab for 45 min on ice in the dark, washed, fixed, and analyzed by flow cytometry.

Conjugation: Abs were conjugated via lysine residues to the potent anti-microtubule maytansine derivative DM4 using a *N*-succinimidyl 4-(2-pyridylthio)-2-sulfobutanoate (sSPDB) linker with a drug-to-antibody ratio of ~3.5. Similarly, Abs were conjugated to the novel tripeptide L-DM21 via *N*-maleimidobutyryl-oxysulfosuccinimide ester (sGMBS) linker with a drug-to-antibody ratio of ~3.5. As a comparator, Ab-vc-MMAE was prepared by reducing interchain disulfide bonds with TCEP and titrating mc-vc-PAB-MMAE to give ~3.5 DAR.

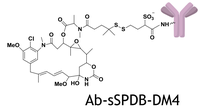

Ab-sSPDB-DM4

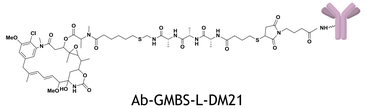

Ab-GMBS-L-DM21

In vitro cytotoxicity assays: To test the cytotoxicity of anti-cMet ADCs, target cells were plated at 2,000 cells per well in 100 µL in complete RPMI media and test article added in a 1:4 dilution series. Cells were incubated for 5 days and viability of remaining cells was determined by WST-8 assay.

In vivo xenograft studies: The antitumor activity of varying doses of ADC was evaluated in female C.B-17 SCID mice bearing xenograft tumors. Test articles were administered as a single i.v. bolus with tumor volume (TV) and body weight (BW) measurements recorded twice per week. All treatments were well tolerated at the indicated doses, and no body weight loss was observed.

In vitro signaling assays: Proliferation, pAKT and pERK

To assess potential agonist activity, anti-cMet Abs were tested in cell proliferation and down-stream signaling assays as described.

- hu5D5 and hu5D5-F'ab serve as positive and negative controls; hu224G11 and hu36C4 as reference.
- hucMet27Gv1.3Hinge variant demonstrates no/ low levels of agonistic activity in all three assays.

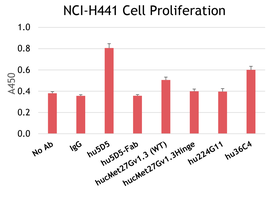

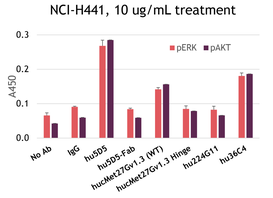

In vitro safety assessments: Hu/cyno ECD and hepatocyte binding

As a safety measure we wanted to ensure our lead Abs had comparable binding to human and cyno cMET EDC to enable NHP tolerability studies.

- hucMet27Gv1.3 WT and Hinge Abs have comparable binding profiles to human and cyno ECD.

Liver hypertrophy has been observed clinically in some MET-targeting agents. We assessed potential binding to normal liver cells as a safety check.

- Compared with EBC-1 cells, lead Abs had low binding to primary human and cyno hepatocytes.

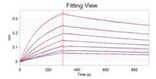

hucMet27Gv1.3Hinge, human cMet ECD

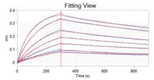

hucMet27Gv1.3Hinge, cyno cMet ECD

Anti-cMet Ab	Human cMet-ECD-his			Cyno cMet-ECD-his		
	KD (M)	K_{on} (1/Ms)	K_{dis} (1/s)	KD (M)	K_{on} (1/Ms)	K_{dis} (1/s)
hucMet27Gv1.3 (WT)	1.82E-09	2.12E+05	3.81E-04	1.71E-09	2.63E+05	4.57E-04
hucMet27Gv1.3Hinge	1.96E-09	2.30E+05	4.51E-04	1.68E-09	3.36E+05	5.64E-04
hucMet224G11	1.47E-09	1.61E+05	2.37E-04	1.11E-09	2.36E+05	1.40E-04

FACS binding to human hepatocytes

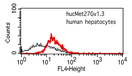

FACS binding to cyno hepatocytes

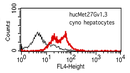

FACS binding to EBC-1 cells

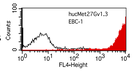

In vitro conjugate binding and cytotoxicity

Anti-cMet-sSPDB-DM4 and -L-DM21 conjugates are highly and selectively cytotoxic on *MET*-amplified cell lines.

- Conjugation does not effect binding.
- cMet-targeting ADCs are highly potent.
- Non-targeting IgG ADCs are not potent.

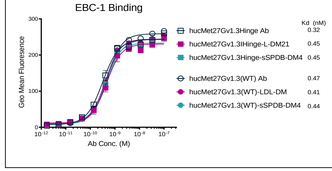

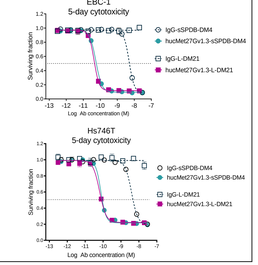

In vivo efficacy and PK of WT vs. Hinge-modified ADCs

hucMet27Gv1.3-sSPDB-DM4 ADCs conjugated to the parental (WT) or the Hinge variant Ab have similar activity in EBC-1 (NSCLC) and Hs746T (gastric) xenograft models.

- ADCs are highly active at low doses with many tumor-fee survivors (TFS) at study end.
  - Complete responses (CRs) seen at 1.25 mg/kg in EBC-1 and 2.5 mg/kg in Hs746T.

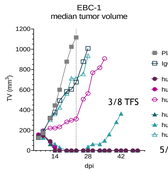

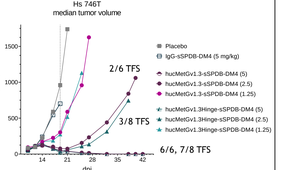

Plasma taken from mice after hucMet27Gv1.3-(WT or Hinge)-sSPDB-DM4 treatment shows similar T_{Ab} and T_{ADC} clearance and similar WT and Hinge values.

- Ab is cross-reactive to tumor, not mouse tissue; n=3 mice per sample.

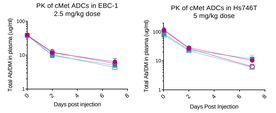

In vivo ADC activity in *MET*-amplified models

hucMet27Gv1.3-sSPDB-DM4 and -L-DM21 conjugates are highly active in EBC-1 (NSCLC) and Hs746T (gastric) *MET*-amplified xenograft models.

- L-DM21 demonstrates an advantage over sSPDB-DM4.

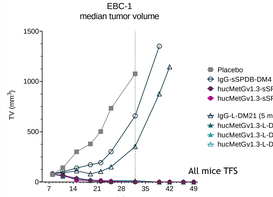

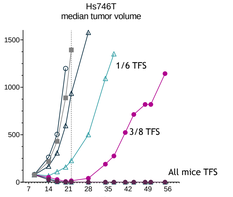

cMet-DM21 is active in non-amplified models

hucMet27Gv1.3Hinge-L-DM21 shows superior activity compared to -sSPDB-DM4 and -vc-MMAE in cMet over-expressing Detroit 562 (SCHNN) and NCI-H441 (NSCLC) xenograft models.

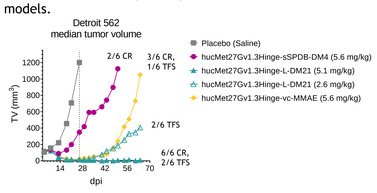

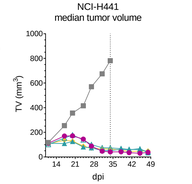

ADCs administered by matching payload dose: 50 µg/kg = 2.6 mg/kg Ab, 100 µg/kg = 5.1- 5.6 mg/kg Ab

CONCLUSIONS

- hucMet27Gv1.3Hinge Ab shows low/no agonism in *in vitro* cell proliferation and signaling assays
- hucMet27Gv1.3Hinge Ab is cross-reactive to human/cyno and shows low binding to hepatocytes
- hucMet27Gv1.3 parental and Hinge-sSPDB-DM4 ADCs are comparably active in *MET*-amplified xenograft models and are stable in circulation
- hucMet27Gv1.3-sSPDB-DM4 and -L-DM21 ADCs are highly active in *MET*-amplified xenograft models with many tumor-free survivors
- hucMet27Gv1.3Hinge-L-DM21 is highly active in Detroit 562 and NCI-H441 non-amplified MET xenograft models

These data demonstrate compelling cMet-targeted activity of the novel non-agonist hucMet27Gv1.3Hinge-L-DM21 ADC.